Energetics of Bulk and Nano-Akaganeite, β-FeOOH: Enthalpy of Formation, Surface Enthalpy, and Enthalpy of Water Adsorption

Lena Mazeina, Suraj Deore, and Alexandra Navrotsky*

Thermochemistry Facility and NEAT ORU, University of California at Davis, One Shields Avenue, Davis, California 95616

Received November 17, 2005. Revised Manuscript Received January 25, 2006

Akaganeite, β-FeOOH, is a commonly occurring ferric mineral in the environment and is a sorbent, ion exchanger, and catalyst. It is often fine-grained (nanophase) and frequently contains excess water. Its enthalpy of formation was studied by solution calorimetry in aqueous HCl. The enthalpy of water adsorption was studied by a new calorimetric technique combining a Calvet microcalorimeter and an automated gas dosing system, used for surface adsorption measurements. Akaganeite samples with surface areas of 30−280 m^2/g were used. Sample characterization was performed by X-ray powder diffraction, Fourier transform infrared spectroscopy, thermogravimetric analysis, Brunauer−Emmett−Teller method, scanning electron microscopy, and transmission electron microscopy. Surface enthalpy and enthalpy of water adsorption are reported for the first time. By adsorbing water, akaganeite decreases its effective surface enthalpy from 0.44 J/m^2 to 0.34 J/m^2. The enthalpy of formation of akaganeite can vary by 10−12 kJ/mol as a function of the surface area. The standard enthalpy of formation of akaganeite with zero surface area was refined and is −554.7 ± 1.9 kJ/mol. Thus, the standard enthalpy of formation and surface enthalpy of akaganeite are between those of goethite and lepidocrocite. The more metastable the polymorph, the lower its surface energy.

Introduction

Although akaganeite has attracted much study because of its unique sorption,[1−3] ion exchange,[4,5] and catalytic properties,[6,7] a thermodynamic description of nano-akaganeite, β-FeOOH, is still lacking. The only known measurement of the enthalpy of formation of bulk akaganeite[8] was made without emphasis on particle size.

Being present in the environment mostly as fine-grained material, akaganeite always has a significant surface area and some amount of excess water, which increases tremendously with decreasing particle size. By adsorbing water, the surface tends to decrease its total excess enthalpy.[9] Such water adsorption complicates the determination and interpretation of the thermodynamic properties of nanophases.[10] The assumption that adsorbed water behaves thermodynamically as bulk liquid water is a good first approximation[11,12] but sometimes leads to contradictory observations in natural systems.[10] At the same time, adsorbed water may inhibit the oxide surface from undergoing other ion-exchange reactions. Knowing the energetics of bound surface water is necessary to interpret calorimetric data, to obtain the thermodynamic properties of the dehydrated surface, and to understand the surface and ion-exchange properties of the material.

Our work addresses the effect of surface area on the thermodynamic stability of akaganeite. The dependence of energetics of akaganeite on particle size is considered for the first time. We obtained the formation enthalpy of akaganeite samples with particle sizes from bulk (>100 nm) to 5 nm by solution calorimetry. Water adsorption calorimetric experiments on bulk and nano-akaganeite were performed as well. The enthalpy of water adsorption thus obtained was used to correct calorimetric data and to calculate the surface enthalpy of the "dry" (water free) akaganeite surface.

Experimental Section

Synthesis. Akaganeite was synthesized in the particle size range 5−100 nm. Most syntheses were performed by hydrolysis of Fe^{3+} solution (100 mL in plastic bottles) at 90 °C.[13] For several samples, urotropin, acting as a particle size-controlling agent,[13] was used. The summary of experimental conditions is shown in Table 1.

* Corresponding author. E-mail: anavrotsky@ucdavis.edu.

(1) Lazaridis, N. K.; Bakoyannakis, D. N.; Deliyanni, E. A. *Chemosphere* **2004**, *58*, 65.
(2) Deliyanni, E A.; Bakoyannakis, D N.; Zouboulis, A I.; Matis, K A. *Chemosphere* **2003**, *50*, 155.
(3) Solozhenkin, P. M.; Deliyanin, E. A.; Bakoyannakis, V. N.; Zouboulis, A. I.; Matis, K. A. *Fiz.−Tekh. Probl. Razrab. Polezn. Iskop.* **2003**, *3*, 92.
(4) Gossuin, Y.; Colet, J.-M.; Roch, A.; Muller, R. N.; Gillis, P. *J. Magn. Reson.* **2002**, *157*, 132.
(5) Cai, J.; Liu, J.; Gao, Z.; Navrotsky, A.; Suib, S. L. *Chem. Mater.* **2001**, *13*, 4595.
(6) Holm, N. G. *Origins Life* **1984**, *14*, 343.
(7) Linehan, J. C.; Matson, D. W.; Darab, J. G. *Energy Fuels* **1994**, *8*, 56.
(8) Laberty, C.; Navrotsky, A. *Geochim. Cosmochim. Acta* **1998**, *62*, 2905.
(9) Jura, G.; Harkins, W. D. *J. Am. Chem. Soc.* **1944**, *66*, 1356.
(10) Navrotsky, A. *Rev. Mineral. Geochem.* **2001**, *44*, 73.
(11) Majzlan, J.; Navrotsky, A.; Casey, W. H. *Clays Clay Miner.* **2000**, *48*, 699.
(12) Mazeina, L.; Navrotsky, A. *Clays Clay Miner.* **2005**, *53*, 113.
(13) Music, S.; Saric, A.; Popovic, S. *J. Mol. Struct.* **1997**, *410/411*, 153.

10.1021/cm052543j CCC: $33.50
Published on Web 03/03/2006

Table 1. Conditions of Akaganeite Syntheses with Urotropin

	initial Fe^{3+}, M	urotropin added, g	duration of hydrolysis at 90 °C, h
AK-102	0.1	0.07	5
AK-134	0.1	0.35	5
AK-166	0.1	0.7	5
AK-280	0.1	1.4	5
AK-92	0.1		5
AK-105	0.1	0.217	24
AK-97	0.1	0.15	24
AK-59	0.1	0.0756	24
AK-86	0.1	0.0289	24
AK-34	0.1		24
AK-43	0.25		24
AK-66	0.5		24
AK-53		see text	
AK-150		see text	

Akaganeite 10 nm in size (AK-150) was prepared by hydrolysis (8 days at 25 °C and then 8 days at 70 °C) of a 1 M $FeCl_3$ solution by addition of 1 M NaOH.[14] Bulk akaganeite (AK-53) was obtained by keeping the 0.1 M $FeCl_3$ solution at 40 °C for 8 days.[14] After precipitation the solids were decanted, dialyzed for 2 weeks using VISKING dialysis tubing, type 36/32, changing the water twice a day, and then freeze dried. After freeze drying, the samples were analyzed without further treatment.

Characterization. Crystal structure was determined by X-ray powder diffraction (XRD) analysis using a Scintag PAD V diffractometer operating at 45 kV and 40 mA with Cu Kα (λ = 1.54056 Å) radiation. The diffractometer was calibrated using quartz as a standard. Patterns were collected from 10 to 70° 2θ angle with a step size of 0.02° and dwell time of 15 s for fine-grained samples and 2 s for coarse-grained samples. Lattice parameters and the size of the diffraction domain (crystallite size) of the samples were determined by Rietveld refinement using JADE 6.1 (Materials Data, Inc., 2001) and Materials Studio 3.2 (Accelrys, Inc., 2004) software. We calculated the tunnel fraction occupied by water molecules in the following way. Each unit cell contains one tunnel in the body (internal) and shares four tunnels at the corners with four other unit cells. At the particle edge there are also some exposed tunnel fragments, which are not shared with any other unit cell. As the particle size decreases, more tunnels become exposed and the fraction of internal tunnels decreases. We calculated the fraction of unexposed tunnels as a function of the surface area of the particle. We assumed that the exposed tunnel fragments do not contain bound water and all internal tunnels are 100% occupied by water. Thus, the water carrying capacity decreases with increasing surface area. The theoretical number of unit cells for akaganeite with different particle sizes was calculated by the ratio of the volume of the particle to the volume of the unit cell (335.4 $Å^3$) for bulk akaganeite. Thus, the obtained water content was plotted as function of calculated surface area (obtained by considering the particles as cubes) in Figure 2. Using the real geometry of the samples would be difficult because we do not know the detailed morphology and what edges are at the particle surface. Therefore, we used a simple geometrical model of exposed tunnels to calculate the tunnel water content as a function of particle size. Usage of the calculated surface area in Figure 2 brings some uncertainty, but so would doing the calculation of available tunnels using an assumed geometry and measured surface area.

Fourier transform infrared (FTIR) spectra were collected with a Bruker Equinox 55 spectrometer using the KBr pellet technique. The FTIR spectra were recorded immediately after pellet preparation. The spectrometer was flushed continuously with nitrogen to avoid contamination by atmospheric water and CO_2 during analysis. Spectra were collected in the 400−4000 cm^{-1} range with a resolution of 4 cm^{-1}. A baseline correction was applied before interpretation.

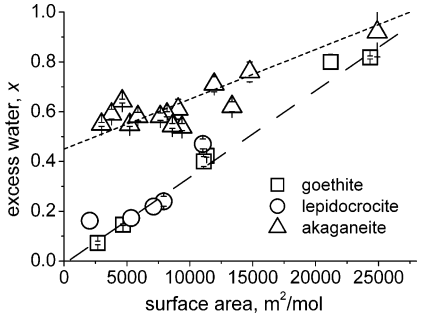

Figure 1. Correlation between surface area of FeOOH and amount of adsorbed water for goethite (α-FeOOH),[12] akaganeite (β-FeOOH), and lepidocrocite (γ-FeOOH).[34] Error bars do not exceed the size of the data symbols.

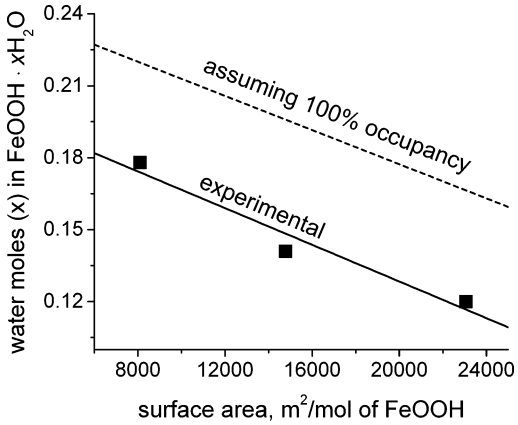

Figure 2. Water remaining after degassing at 150 °C. Dashed line: calculated assuming 100% tunnel occupancy by water molecules (see text). Solid line: least-squares regression of the experimental data.

Chloride content was analyzed commercially (Galbraith Laboratories). Excess water content was determined in a furnace experiment by heating the samples at 1050 °C for 12 h. The amount of adsorbed water was calculated from the total weight loss over the stoichiometric weight loss (10.14 wt %) for the reaction

$$\beta\text{-FeOOH} = \frac{1}{2}\alpha\text{-}Fe_2O_3 + \frac{1}{2}H_2O \qquad (1)$$

The chlorine content was neglected while calculating the excess water because of its very low value.

The surface area was measured by the BET (Brunauer−Emmett−Teller) method[15] on a Micromeritics ASAP 2020 apparatus. Samples were vacuum degassed at 60 °C for at least 10 h.

Scanning electron microscopy (SEM; on a FEI XL30-SFEG instrument) and high-resolution transmission electron microscopy (HRTEM; on a Topcon 002b instrument, at the National Center for Electron Microscopy, Lawrence Berkeley National Laboratory) micrographs were taken to determine the morphology and crystal sizes of akaganeite. HRTEM analysis was performed using a LaB_6 filament at 200 kV, using a carbon black standard Ted Pella #645 for calibration.

Results of sample analyses are given in Table 2.

Calorimetric Measurements. The enthalpy of solution ΔH_{sln} was measured in a Hart Scientific IMC-4400 isothermal calorimeter. Experiments were performed at 25 and 70 °C using HCl (5.0 N

(14) Schwertmann, U.; Cornell, R. M. *The iron oxides in the laboratory: preparation and characterization*; VCH: New York, 2000.

Table 2. Surface Areas and Excess Water and Chloride Contents of Nano- and Bulk Akaganeite Samples

sample ID[a]	surface area, m^2/g	crystallite size, nm (XRD)	particle size, nm (SEM/TEM)	weight loss on ignition, %	excess water, *x*, in $FeOOH \cdot xH_2O$	Cl content, *y*, in $FeOOH \cdot xH_2O \cdot yCl$
AK-280	279.7 ± 1.5	4.5	4 × 4 crystals	22.9 (1)	0.82	0.0035
AK-166	165.9 ± 0.7	7.6		22.4[b] ± 0.5[c] (6)[d]	0.78 ± 0.04	0.0046
AK-150	150.5 ± 0.6			20.4 ± 0.2 (6)	0.64 ± 0.02	0.00003
AK-134	134.1 ± 0.6	8.4	rods 9 × 160	21.5 ± 0.4 (6)	0.72 ± 0.03	0.0054
AK-105	105.4 ± 1.0	15		19.0 ± 0.2 (7)	0.54 ± 0.01	*e*
AK-102	102.1 ± 0.6	15		20.2 ± 0.7 (6)	0.60 ± 0.01	0.0033
AK-97	96.8 ± 1.0			19.1 ± 0.1 (7)	0.55 ± 0.01	*e*
AK-92	92.2 ± 2.5	18[f]	rods 10 × 50 somatoids 50 × 200[f]	20.1 ± 0.2 (5)	0.60 ± 0.02	0.0045
AK-86	86.0 ± 0.8	20		19.7 ± 0.2 (6)	0.59 ± 0.02	*e*
AK-66	66.0 ± 0.8			19.7 ± 0.3 (6)	0.59 ± 0.02	*e*
AK-59	58.7 ± 0.6	35		19.2 ± 0.1 (6)	0.553 ± 0.008	*e*
AK-53	52.6 ± 1.3	>100	rods 90 × 400	20.7 ± 0.1 (6)	0.661 ± 0.008	0.004
AK-43	42.5 ± 0.6	>100		19.9 ± 0.3 (6)	0.60 ± 0.02	*e*
AK-34	33.5 ± 0.5	>100		19.2 ± 0.1 (6)	0.555 ± 0.01	*e*

[a] Samples IDs are given according to obtained surface area in m^2/g measured with activation temperature 60 °C. [b] Average. [c] Two standard deviations of the mean. [d] Number of measurements. [e] Not analyzed. [f] The sample contains particles with different shapes and sizes.

standardized solution, Alfa Aesar). Calorimeter calibration was performed by dissolving KCl (NIST standard reference material 1655) in deionized water at 25 °C. The average sample weight was about 5 mg. For a better calorimetric signal and to accelerate the dissolution, the solutions were stirred mechanically at ~60 min^{-1}. The measured heat effect of ΔH_{sln} is the sum of the heat of solution and heat content of the sample. To determine the heat content ΔH_{ttd} at 70 °C, transposed temperature drops of several akaganeite samples and also of bulk hematite were collected by dropping pellets into an empty crucible at 70 °C. At the end of the transposed temperature drop experiments, the pellets were collected and analyzed for the remaining excess water by heating the pellets at 1050 °C.

Water adsorption calorimetric experiments were performed for several samples. The technique combines precision gas dosing and volumetric detection of amount of adsorbed gas (by Micromeritics ASAP 2020) with commercial Calvet type microcalorimeter (SETARAM DSC111).[16] Before the water adsorption experiment, samples were degassed at 150 °C for at least 10 h. The remaining water was determined from the weight loss of the sample during degassing (by subtracting from the total excess water content) and additionally by heating the sample at 1050 °C (as described above). Phase purity after degassing was checked by XRD and FTIR. Spectra were analyzed for the presence of other phases and compared with the spectra before degassing. After degassing, the full isotherm, including BET surface area, porosity, and free volume of the sample tube, was measured. After BET measurements, the samples were evacuated. The criterion of sufficient sample degassing was the sample leak rate of <0.6 μm Hg/min at 25 °C. Water vapor was introduced in a series of small dosing steps. The heat of adsorption of each dose was recorded by a calorimeter operated at 25 °C. Thus a simultaneous record of enthalpy, dose, and adsorption isotherm was obtained. The area A_i of each calorimetric peak was measured, and the heat effect Q_i was calculated using the enthalpy of fusion of Ga as the calibration factor *k*: $Q_i = kA_i$. The heat effect Q_i was then divided by the corresponding dose w_i of adsorbed water, thus giving the differential enthalpy of adsorption:

$$H_i^{dif} = \frac{Q_i}{w_i} \tag{2}$$

The integral enthalpy at a given coverage *j* is the sum of the heats Q_i divided by the total amount of adsorbed water up to the given coverage *j*:

$$H_j^{int} = \sum_1^j Q_i / \sum_1^j w_i \tag{3}$$

After each water adsorption experiment the samples were additionally analyzed by XRD and FTIR. To check reproducibility of the water adsorption experiments, we performed two consecutive runs with the sample AK-43 and then repeated the experiments with a fresh portion of the sample.

Results

Characterization. XRD and FTIR analyses revealed that all samples were pure β-FeOOH without admixtures of organics, iron hydroxide, or other phases. Structural refinement showed that synthetic akaganeite undergoes some transformation (symmetry decreasing) with decreasing particle size. Detailed description of structural analysis will be given in a separate paper.

The BET surface area measured with degassing at 60 °C (Table 2) is lower than that measured with degassing at 150 °C (Table 5). The calculation converting from m^2/g to m^2/mol was made assuming stoichiometric β-FeOOH. Full isotherm data for the samples degassed at 150 °C revealed micropores, which caused the increase of total BET surface area. Because the general trend in surface area obtained for samples activated at 60 °C agrees with the crystallinity and particle size trends observed in XRD data, in all plots, we used the BET surface area, obtained from the samples degassed at 60 °C. Detail discussion of micropore size, ratios between external and internal micropore surface area, and dependence of surface area on the activation temperature was beyond the scope of the article and can be found elsewhere.[18]

Results of the loss on ignition experiments and the excess water content are shown in Table 2. Weight loss experiments showed increasing excess water as particle size decreases (Figure 1). Water content remaining after degas is plotted versus surface area together with calculated tunnel water content (Figure 2). Though this calculation is approximate, it illustrates the general behavior observed.

(15) Brunauer, S.; Emmett, P. H.; Teller, E. *J. Am. Chem. Soc.* **1938**, *60*, 309.
(16) Ushakov, S. V.; Navrotsky, A. *Appl. Phys. Lett.* **2005**, *87*, 164103.

Table 3. Calorimetric Data

sample ID	surface area, $m^2 \cdot 10^3$/mol	ΔH_{sln},[a] 25 °C, kJ/mol	ΔH_{sln},[a] 70 °C, kJ/mol	ΔH_{ttd},[a] 70 °C, kJ/mol
AK-280	24.9	−47.2 ± 0.6	−30.2 ± 0.5 (3)	10.5 ± 0.8 (4)
AK-166	14.8	−43.7 ± 0.6	−20.5 ± 0.5 (3)	10.0 ± 0.3 (4)
AK-150	13.5	−41.8 ± 0.6	−20.25 ± 0.4 (3)	
AK-134	12.0	−42.8± 0.4	−20.6 ± 0.6 (3)	9.8 ± 0.5 (3)
AK-105	9.4	−41.3 ± 0.8		
AK-102	9.1	−41.6 ± 0.3		
AK-97	8.5	−41.7 ± 0.2		
AK-92	8.2	−41.4 ± 1.2		
AK-86	7.6	−41.3 ± 0.6		8.8 ± 1.2 (7)
AK-66	5.9	*b*	−19.4 ± 0.8 (3)	
AK-59	5.2	−40.6 ± 0.9	−20.8 ± 0.3 (3)	
AK-53	4.6	−11.5 ± 0.7 (3)[c]	−19.6 ± 1.5 (5)	7.7 ± 0.3 (4)
AK-43	3.8	9.0 (1)[c]	−18.7 ± 1.4 (3)	
AK-34	3.0	−6.3 ± 0.2 (5)[c]	−21.4 ± 1.1 (5)	
intercept	0.0	−41.3 ± 1.3	−21.9 ± 1.9	6.6 ± 1.9

[a] sln = solution; ttd = transposed temperature drop. [b] It was not possible to obtain the heat of solution because of very slow dissolution. [c] Very slow dissolution with the big baseline shift.

Table 4. Thermodynamic Cycle and Reference Calorimetric Data for Calculation of Enthalpy of Formation, ΔH_f, of Akaganeite Using Acid Calorimetry Performed at 25 °C and 70 °C. All data are in kJ/mol[a]

reaction	enthalpy of reaction
General Reactions	
	$\Delta H_1 = \Delta H_f°(\beta\text{-FeOOH})$
$Fe_{cr} + (0.5n + 1)O_2(g) + (n + {}^1/_2)H_2(g) = \beta\text{-FeOOH}_{cr}\{\cdot nH_2O_{str}\}$	$\Delta H_1' = \Delta H_f°(\beta\text{-FeOOH}\cdot nH_2O) = \Delta H_1 + n\Delta H_4$
$\beta\text{-FeOOH}_{cr}\cdot nH_2O_{str} + (x - n)H_2O(g) = [\beta\text{-FeOOH}_{cr}\cdot nH_2O_{str}\cdot(x - n)H_2O_{ads}]$	$\Delta H_2 = \Delta H_{ads}$
$H_2O(l)_{25°C} = H_2O(g)_{25°C}$	$\Delta H_3 = 44.0$[20]
$H_2(g)_{25°C} + {}^1/_2O_2(g)_{25°C} = H_2O(l)_{25°C}$	$\Delta H_4 = \Delta H_f°(H_2O) = -285.8 \pm 0.1$[20]
adsorption enthalpy relative to liquid water	$\Delta H_5 = \Delta H_2 + \Delta H_3 = -15.0 \pm 1.1$
25 °C	
$[\beta\text{-FeOOH}_{cr}\cdot nH_2O_{str}\cdot(x - n)H_2O_{ads}] + [3H^+](aq) = [Fe^{3+} + (2 + x)H_2O](aq)$	$\Delta H_6 = \Delta H_{sln}(\beta\text{-FeOOH}\cdot xH_2O)$
$\gamma\text{-FeOOH}_{cr,25°C} + [3H^+](aq)_{25°C} = [Fe^{3+} + 2H_2O](aq)$	$\Delta H_7 = \Delta H_{sln}(\gamma\text{-FeOOH}) = -46.5 \pm 0.2$[23]
$Fe_{cr} + O_2(g) + {}^1/_2H_2(g) = \gamma\text{-FeOOH}_{cr}$	$\Delta H_8 = \Delta H_f°(\gamma\text{-FeOOH}) = -549.4 \pm 1.4$[22]
$H_2O(l)_{25°C} = H_2O(aq)_{25°C}$	$\Delta H_9 = \Delta H_{dilution} = -0.4$[23]
$\Delta H_1 = -\Delta H_6 + \Delta H_7 + \Delta H_8 + x\Delta H_9 - m\Delta H_5$	
70 °C	
$[\beta\text{-FeOOH}_{cr}\cdot nH_2O_{str}(x - n)\cdot H_2O_{ads}]_{25°C} + [3H^+](aq)_{70°C} = [Fe^{3+} + (2 + x)H_2O](aq)_{70°C}$	$\Delta H_{10} = \Delta H_{sln}(\beta\text{-FeOOH}\cdot xH_2O)$
$\alpha\text{-FeOOH}_{cr,25°C} + [3H^+](aq)_{70°C} = [Fe^{3+} + 2H_2O](aq)_{70°C}$	$\Delta H_{11} = \Delta H_{sln}(\alpha\text{-FeOOH}) = -16.3 \pm 0.8$
$Fe_{cr,25°C} + O_2(g)_{25°C} + {}^1/_2H_2(g)_{25°C} = \alpha\text{-FeOOH}_{cr,25°C}$	$\Delta H_{12} = \Delta H_f°(\alpha\text{-FeOOH}) -560.1 \pm 1.4$[12]
$H_2O(l)_{70°C} = H_2O(aq)_{70°C}$	$\Delta H_{13} = \Delta H_{dilution} = -0.5$[23]
$H_2O(l)_{25°C} = H_2O(l)_{70°C}$	ΔH_{14} = heat content = 3.4
$\alpha\text{-Fe}_2O_{3\ cr,25°C} + [6H^+](aq)_{70°C} = [2Fe^{3+} + 3H_2O](aq)_{70°C}$	$\Delta H_{15} = \Delta H_{sln}(\alpha\text{-Fe}_2O_3) = -42.3 \pm 2.4$
$Fe_{cr,25°C} + O_2(g)_{25°C} + {}^1/_2H_2(g)_{25°C} = \alpha\text{-FeOOH}_{cr,25°C}$	$\Delta H_{16} = \Delta H_f°(\alpha\text{-FeOOH}) = -826.2 \pm 1.3$[20]
$\Delta H_1 = -\Delta H_{10} + \Delta H_{11} + \Delta H_{12} + x\Delta H_{13} + x\Delta H_{14} - m\Delta H_5 -$ goethite as reference phase	
$\Delta H_1 = -\Delta H_{10} + 0.5\Delta H_{15} + 0.5\Delta H_{16} + (x + 0.5)\Delta H_{13} + (x + 0.5)\Delta H_{14} + 0.5\Delta H_4 - m\Delta H_5 -$ hematite as reference phase	

[a] m = "chemically adsorbed water"; n = water remaining after degassing; and x = total excess water.

Water Adsorption Calorimetry. For an accurate measurement of water adsorption energetics it is critical for the surface of the material to be as dry as possible. Therefore, it was important to find the maximum temperature at which akaganeite loses the most excess water but does not transform to other phases. Our tests and literature data[17−19] showed that 150 °C is optimum: no evidence of structural change was obtained by FTIR or XRD. We thus chose degassing at 150 °C as standard conditions for all samples.

Water adsorption isotherms were recorded until $P/P_0 = 0.2-0.4$. Isotherms can be fit to the Frenkel−Halsey−Hill equation[29,32]

$$\log \frac{P_0}{P} = \frac{A}{\theta^s} \tag{4}$$

where P/P_0 is relative pressure, A is a constant, θ is surface coverage in H_2O/nm^2, and s is an exponent "based upon the decay of surface forces with distance".[28] Surface coverage θ in H_2O/nm^2 was calculated as following

$$\theta = \frac{q_{ads} V_{H_2O} m N_A}{SA} \tag{5}$$

where q_{ads} is a quantity of adsorbed water (experimental data) in cm^3/g, V_{H_2O} is molar volume of 1 cm^3 of H_2O equal to 4.46×10^{-5} mol/cm^3, N_A is Avogadro's constant, and m and SA are mass (in g) and total surface area of sample in nm^2 (of the sample activated at 150 °C), respectively. For the purpose of curve fitting, eq 4 is put in the form

$$\log\left[\log \frac{P_0}{P}\right] = -s \log \theta + A^* \tag{6}$$

Thus, the s constants were evaluated from the slope of the

(17) Gonzalez-Calbet, J. M.; Alario-Franco, M. A.; Gayoso-Andrade, M. *J. Inorg. Nucl. Chem.* **1981**, *43*, 257.
(18) Cornell, R. M.; Schwertmann, U. *The iron oxides: structure, properties, reactions, occurrence and uses*; VCH: Weinheim: Germany, 1996.
(19) Chambaere, D. G.; De Grave, E. *Phys. Chem. Miner.* **1985**, *12*, 176.
(20) Robie, R. A.; Hemingway, B. S. *U.S. Geological Survey Bulletin*; 2131; U.S. Geological Survey: Reston, VA, 1995.
(21) Majzlan, J.; Lang, B. E.; Stevens, R.; Navrotsky, A.; Woodfield, B. F.; Boerio-Goates, J. *Am. Mineral.* **2003**, *88*, 846.
(22) Majzlan, J.; Grevel, K. D.; Navrotsky, A. *Am. Mineral.* **2003**, *88*, 855.
(23) Majzlan, J.; Navrotsky, A.; Schwertmann, U. *Geochim. Cosmochim. Acta* **2004**, *68*, 1049.
(24) Tagirov, B. R.; Diakonov, I. I.; Devina, O. A.; Zotov, A. V. *Chem. Geol.* **2000**, *162*, 193.
(25) Naono, H.; Sonoda, J.; Oka, K.; Hakuman, M. *Stud. Surf. Sci. Catal.* **1993**, *80*, 467.
(26) Post, J. E.; Heaney, P. J.; Von Dreele, R. B.; Hanson, J. C. *Am. Mineral.* **2003**, *88*, 782.
(27) Harkins, Wm. D.; Jura, G. *J. Am. Chem. Soc.* **1944**, *66*, 919.
(28) Halsey, G. *J. Chem. Phys.* **1948**, *16*, 931.
(29) Carey, J. W.; Navrotsky, A. *Am. Mineral.* **1992**, *77*, 930.
(30) Kiseleva, I.; Navrotsky, A.; Belitsky, I. A.; Fursenko, B. A. *Am. Mineral.* **1996**, *81*, 658.

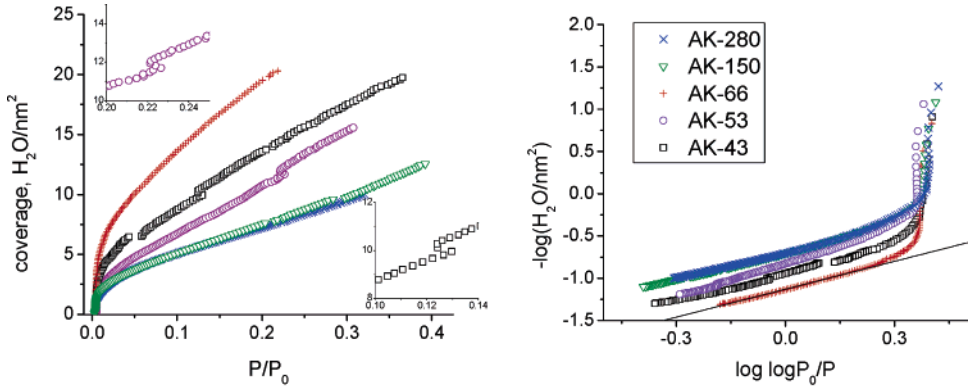

Figure 3. Adsorption of water on akaganeite having different particle sizes. (a) Samples AK-53 and AK-43 show steps at $P/P_0 \sim 0.23$ and ~ 0.13, respectively. (b) Isotherms from $P/P_0 = 0.016$ to $\sim 0.2-0.35$ can be linearly fitted according to eq 4 with the slopes $s = 0.7-0.92$; the straight line shows an example of the fitting. Symbol designations are the same for both diagrams.

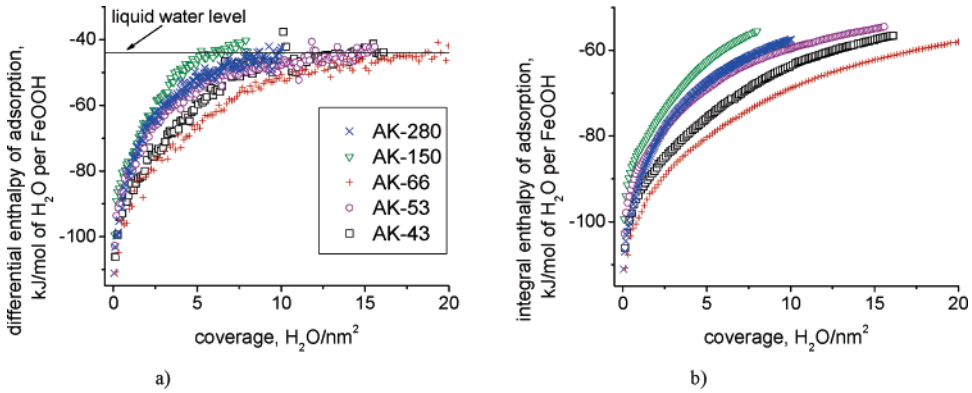

Figure 4. Differential (a) and integral (b) enthalpies of water adsorption as a function of H_2O coverage of the surface. Symbol designations are the same for both diagrams.

Table 5. Results of Water Adsorption Calorimetry

		excess water			integral ΔH_{ads}, kJ/mol of H_2O per FeOOH			
			remaining after degassing					
sample ID	BET surface area,[a] m^2/g	total, H_2O/nm^2	n mol/FeOOH	H_2O/nm^2	first dose	at liquid water level	coverage at liquid water level, H_2O/nm^2	% excess water
AK-280	260	21.4	0.12	3.1	−113.1	−58.9 ± 0.7	8.7	41
AK-150	166	25.9	0.141	5.7	−99.4	−60.5 ± 0.6	6.1	23
AK-66	91	43.6	0.178	13.2	−110.9	−59.2 ± 0.6	18.4	42
AK-53	152	29.4	<0.02	<0.03	−102.7	−57.4 ± 0.6	12.1	41
AK-43	111	44.6	<0.01	<0.03	−106.2	−59 ± 0.5	14.2	39
					average	−59.0 ± 1.3		

[a] The activation temperature is 150 °C.

Table 6. Fitting Parameter s of log[log(P_0/P)] as a Function of log θ and Range of Pressure and Coverage of the Fitting

	s	pressure range, P/P_0	coverage range, H_2O/nm^2
AK-280	0.93	0.016−0.32	3.5−10
AK-150	0.92	0.016−0.40	2.4−13
AK-86	0.90	0.016−0.22	6.6−20
AK-53	0.74	0.016−0.31	2.8−15
AK-43	0.92	0.016−0.36	4.4−20

graph at higher P/P_0 values (Figure 3) and are given in Table 6. The linear regression correlation parameter R^2 is >0.99 for all curves. Knowing the value of the s parameter, one can estimate the attraction between adsorbent and adsorbate.[28]

Calorimetric data for water adsorption experiments were collected until the adsorbed water enthalpy reached the value for bulk liquid water, that is, until the differential enthalpy, namely, the enthalpy of adsorption of a specific dose, attained −44 kJ/mol (see Figure 4a). Although we do not know exactly how water is bound on the akaganeite surface, we will call water adsorbed after the "liquid water enthalpy level" as "physically" adsorbed water and that adsorbed before as "chemically" adsorbed water. We will call excess water remaining after degassing at 150 °C "tunnel" water. Repeated water adsorption experiments for the sample AK-53 showed the same enthalpy of water adsorption reaching liquid bulk water energetics at the same surface coverage. Calorimetric data are presented in Figure 5.

Solution Calorimetry. Results of acid calorimetry are shown in Table 3. For each sample, the reported enthalpy (ΔH_{sln} or ΔH_{ttd}) represents the average of several measurements with an associated error of two standard deviations

(31) McClellan, A. L.; Harnsberger, H. F. *J. Colloid Interface Sci.* **1967**, *23*, 577.
(32) Champion, W. M.; Halsey, G. D. *J. Phys. Chem.* **1953**, *57*, 646.

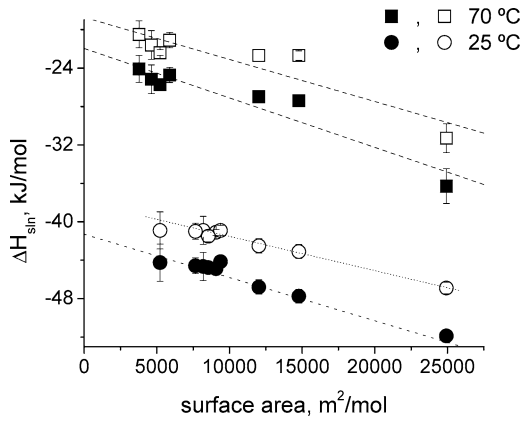

Figure 5. Calorimetric data directly measured (open symbols) and corrected for water (filled symbols) from acid solution calorimetry at 25 and 70 °C (kJ/mol of FeOOH·xH$_2$O for uncorrected data and kJ/mol of FeOOH for corrected data) as a function of the surface area of akaganeite. Dashed lines represent least-squares regression lines.

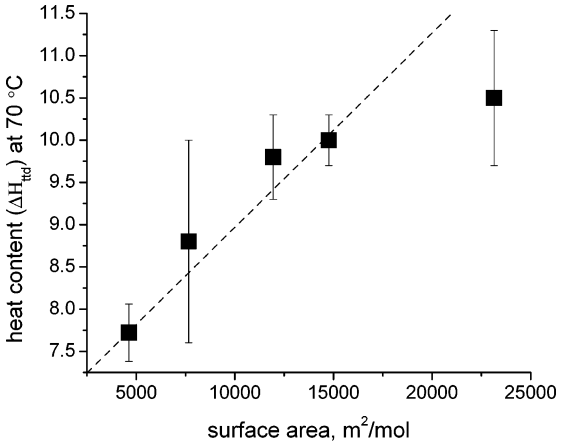

Figure 6. Heat content (ΔH_{ttd} values from Table 3) of akaganeite, in kJ/mol of FeOOH·xH$_2$O as a function of surface area. The heat content of the finest grained sample shows anomalous deviation from the linear dependence of coarser samples.

of the mean. The relationship between ΔH_{sln} or ΔH_{ttd} and surface area is shown in Figures 5 and 6.

ΔH_{ttd} at 70 °C for hematite (4.4 ± 0.4 kJ/mol) agrees with the tabulated heat content of 4.8 kJ/mol[20] within the experimental error; therefore, this method of measuring the heat content is reliable. Furnace weight loss experiments showed that excess water content after the transposed temperature drop experiment is the same within the experimental error as that before; thus, no water evaporated or desorbed from the surface of akaganeite during the drop. Therefore, ΔH_{ttd} at 70 °C for akaganeite represents the heat content of akaganeite with the nominal composition FeOOH plus the heat content of adsorbed water. The intercept of the fitted line with the y axis at $x = 0$ is the heat content of bulk akaganeite with zero surface area and is equal to 6.6 ± 1.9 kJ/mol. This is 3.0 ± 1.9 kJ/mol and 3.2 ± 1.9 kJ/mol higher than the heat contents of goethite and lepidocrocite at 70 °C, respectively.[21]

The thermodynamic cycle for heat of formation, $\Delta H_f°$, calculation from acid calorimetry is given in Table 4. Calorimetric cycles were corrected for excess water, taking into account adsorption enthalpy of "chemically" and "physically" bound excess water. For all calorimetric cycles, chlorine contained in akaganeite was neglected because of its small amount (less than 0.2 wt %) and, therefore, was insignificant input to the total heat effect (less than 0.3 kJ per FeOOH·xH$_2$O). Bulk lepidocrocite[22] and bulk goethite[12] were used as a reference phases for the acid solution experiments at 25 and 70 °C, respectively. In the calorimetric cycle for acid calorimetry we do not specify exact speciation of dissolved Fe^{3+} in 5.0 N HCl. At such a high concentration of HCl, dissolved iron is totally complexed by chloride as $FeCl_2^+$.[24] Because the iron concentration in the solution is very similar for the sample and the reference phase, all chloride complexes of the sample in the calorimetric cycle will be canceled by those of the reference phase. For a cross check of the calorimetric cycle at 70 °C, bulk hematite was also dropped. Because of the large error of ΔH_{sln}, values of ΔH_f of akaganeite calculated using hematite have larger propagated error than values obtained using goethite as a reference phase. Nevertheless, values obtained for the enthalpy of formation, using goethite and hematite as the reference phases, are in a very good agreement (Figure 7).

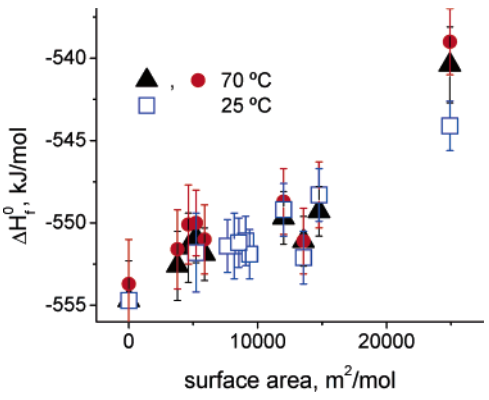

Figure 7. Enthalpy of formation of akaganeite with different particle sizes obtained from acid solution calorimetry at 25 and 70 °C. Circles show enthalpies of formation of akaganeite calculated using hematite as a reference phase, and the other symbols refer to data using lepidocrocite (squares) and goethite (triangles).

To compare results of acid calorimetry at 25 and 70 °C the calculated standard enthalpies of formation from elements $\Delta H_f°$ were plotted versus surface area (Figure 7). Bulk samples (AK-66, AK-43, AK-53, and AK-34) dissolved too slowly at 25 °C for an accurate measurement and the enthalpy of formation was not calculated. Enthalpies of formation obtained from the acid calorimetry data at 25 and 70 °C are in agreement for all measured samples.

The surface enthalpies of water-containing and unhydrated akaganeite are equal to the slopes of the best-fit line of directly measured and corrected data obtained by least-squares regression of the acid calorimetry data at 25 and 70 °C (from Table 3) with the confidence interval of regression set at 0.95 (Figure 5).

Figure 5 shows that several data points corresponding to surface areas less than 10 000 m^2/mol have the same enthalpy of solution within experimental error. This behavior might suggest that these data depart from the linear trend and behave as bulk. Nevertheless, the similar values of enthalpy of solution for those samples are due to the small value of surface enthalpy and, as a consequence, the small contribution of surface enthalpy to total energetics of coarser particles. In general, extrapolation of energy data from the nanoregion

to the bulk region is difficult taking into account the rather complicated structure of akaganeite. The refinement of the akaganeite structure for samples with different particle sizes is in progress. We suspect slight changes in structure, and this might have an effect on the energetics and water content (as in Figure 1). With the current available data, the linear trend in Figure 5 is the only justifiable treatment of the data. The slope of this trend would reflect the average surface enthalpy of the samples over the whole surface area range.

The standard enthalpies of formation for akaganeite with zero surface area and nominal compositions of FeOOH were calculated from the intercepts of the fitted lines (Figure 5) using the corresponding calorimetric cycle.

Discussion

Excess Water. A correlation of the surface area and amount of excess water, *x*, is observed for the akaganeite samples in the particle size range studied. Figure 1 shows that at lower surface areas akaganeite has a significantly higher amount of excess water than the other oxy-hydroxides, goethite and lepidocrocite. Chlorine could occupy only two-thirds of all tunnels,[18] but chlorine content in akaganeite is usually only 2−7 mmol/mol of FeOOH. It is obviously insufficient to fill even two-thirds of the tunnels, whose ideal content is 0.25 mol Cl per FeOOH. Therefore, to maintain the structure, water molecules fill the tunnels.[18,25] This explains the higher excess water, especially for bulk samples (Figure 1) than for other oxyhydroxides. The observation that excess water remains after degassing at 150 °C supports the hypothesis of tunnel water. Complete removal of this tunnel water causes structure collapse[18] and akaganeite transformation to hematite or goethite.[14,18]

Relatively similar water content for samples having surface areas below about 10 000 m^2/mol might suggest a flat rather than a linear trend. It is well-known that akaganeite properties depend very much on many parameters such as synthesis conditions, pore size, and content of excess as well as tunnel water. Variations in one or all of these parameters might cause the scatter in the data in Figure 1 for low surface area samples. Also, slight changes in the structure of akaganeite as a function of all these parameters as well as particle size are not excluded. At the current state of the available data, a linear trend is the only justifiable fit.

A surface area increase of samples activated at 150 °C is attributed to the appearance of micropores.[17] At 150 °C water escapes from tunnels; thus, N_2 can penetrate into the tunnels and micropores can be detected.[25]

When the particle size decreases, the fraction of internal tunnels also decreases and so does the tunnel water content. Figure 2 shows a correlation between the surface area of nano-akaganeite and water remaining after degassing at 150 °C and also a correlation between surface area and calculated tunnel water. The slopes of the experimental data and calculated curves show very good agreement. Therefore, we conclude that remaining excess water after degassing at 150 °C is the tunnel water.

The bulk sample showed no remaining excess water after degassing at 150 °C (see Table 5). Although the tunnel structure of bulk akaganeite is well-known,[18,26] the tunnel structure of the nanoparticles is still not well-constrained. In the bulk samples, the tunnel size and shape allow water molecules to diffuse during degassing. It is possible that in nano-akaganeite the tunnels undergo structural deformations because of the effects associated with their surface terminations. The suspected symmetry change at the nanoscale, seen in XRD and TEM patterns and still under investigation, may also imply some distortion of the tunnels and perhaps less effective water diffusion. Nevertheless, because all excess water can be removed from the bulk samples, the energetics of all excess water can be studied.

Water Adsorption. The main goal of the water adsorption calorimetric experiments was to determine the energetics of bound surface water. The integral enthalpy of water adsorption at the liquid water enthalpy level is the same for all samples independent of surface area and particle size (see Table 5). The main difference is the water coverage at which the differential adsorption enthalpy reaches that of liquid bulk water (−44 kJ/mol; see Figure 4a). Coverage at this liquid water enthalpy level decreases with decreasing particle size (see Table 5). The similar integral adsorption enthalpy (presented as a function of water coverage in Figure 4b) but with different coverage at the liquid water enthalpy level suggests that adsorbed water bonds are similar for all samples and independent of particle size; however, the geometry of the surface is different, and the amount of available sites probably decreases with decreasing particle size. A similar content of "chemically" bound water (∼40 mol % of total water) for almost all samples supports this idea. The average integral enthalpy of water adsorption at the liquid water enthalpy level for all samples is −59.0 ± 1.3 kJ/mol (Table 5). The integral enthalpy of adsorption relative to liquid bulk water, obtained by subtracting −44 kJ/mol from −59.0 kJ/mol, is −15.0 ± 1.3 kJ/mol. This moderate value supports the idea that this water is "chemically" adsorbed but not too strongly bound. For comparison, enthalpies of hydration of zeolites are often near −40 kJ per mole of water.[29,30] This value of −15 kJ/mol was used in the calorimetric cycles to correct calorimetric values for "chemically" adsorbed water assuming $\Delta H_{des} = -\Delta H_{ads}$. Values of the *s* parameter in the Frenkel−Halsey−Hill fitting of akaganeite water adsorption isotherms are in the range 0.76−0.92 (Table 6). When the area of the adsorbed water molecule reported for hematite (10.8 $Å^2$) is used,[31] the corresponding degree of surface coverage on akaganeite would be significantly more than 1. An independent estimate of the area per water molecule would be needed to determine whether the water becomes loosely bound even before a monolayer coverage is attained.

In the case of adsorption on a uniform surface, one would expect a stepwise adsorption isotherm,[32] where each step corresponds to one adsorbed monolayer. No stepwise isotherms were observed in our water adsorption experiments except for two slight steps for AK-43 and AK-53 (see Figure 3). The reason for steps being suppressed and leveling of the adsorption isotherms, even though experiments were certainly performed beyond the monolayer region,[27] is probably the nonuniformity of the akaganeite surface[32] and cooperative adsorption.[28]

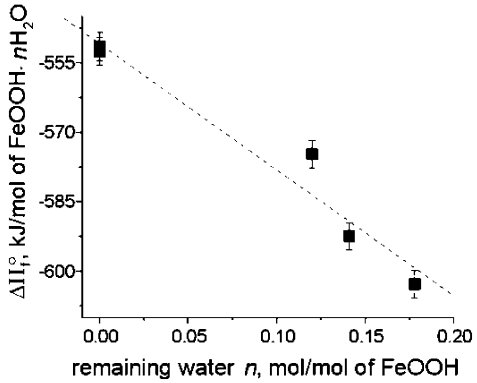

Figure 8. Enthalpy of formation of $FeOOH{\cdot}nH_2O$ as a function of remaining excess water, *n*, after degassing at 150 °C. Dashed line: linear regression of the data with slope of -271 ± 18 kJ/mol.

Table 7. Surface Enthalpy and Standard Enthalpy of Formation of Bulk Akaganeite

		acid calorimetry at 70 °C	acid calorimetry at 25 °C
surface enthalpy, ΔH_s, J/m^2	"dry" (water free) surface	0.51 ± 0.20 ($R^2 = 0.90$)	0.44 ± 0.04 ($R^2 = 0.96$)
	hydrated surface	0.44 ± 0.22 ($R^2 = 0.84$)	0.34 ± 0.04 ($R^2 = 0.96$)
enthalpy of formation, $\Delta H_f°$, kJ/mol		-554.7 ± 2.4	-554.7 ± 1.9

Enthalpy of Formation. The standard enthalpy of formation of akaganeite with zero surface area was calculated from the intercept of the line fitting of calorimetric data, ΔH_{sln}, obtained at 25 °C and at 70 °C, versus surface area (see Figure 5). Both values agree within experimental error (Table 7). The value of -554.7 ± 1.9 kJ/mol is our recommendation of the standard enthalpy of formation of akaganeite with nominal composition FeOOH and zero surface area. Because akaganeite is almost always encountered in the environment as a fine-grained material, the measured values for akaganeites with nonzero surface area are also useful. The only reported value of standard enthalpy of akaganeite is -561.3 ± 2.4 kJ/mol[8] and very close to that of goethite. The present value refines that earlier determination because surface enthalpy, excess water content, and enthalpy of water adsorption are taken into account.

Enthalpy of formation of the samples containing water remaining after degassing at 150 °C was calculated taking into account this excess water as shown in Table 4 and plotted as function of remaining water *n* (Figure 8). The slope of the linear fit of the data (-271 ± 18 kJ/mol) is the same within experimental error as the enthalpy of formation of liquid water (-285.1 kJ/mol). This suggests that tunnel water is weakly bound water and can be considered as physically adsorbed water having bulk liquid water energetics. Considering tunnel water as less strongly adsorbed water than the water on the exposed surface (with the enthalpy of adsorption of -15 kJ/mol) would not change the energetics significantly: a tunnel water content of $0.12-0.18$ multiplied by -15 kJ/mol will contribute only $1.8-2.7$ kJ/mol. Thus, the value of the heat of formation is not very sensitive to the assumption about the nature of the tunnel water.

Surface Enthalpy. The obtained surface enthalpies are 0.51 ± 0.20 J/m^2 (calculated from acid calorimetry at 70 °C) and 0.44 ± 0.04 J/m^2 calculated from acid solution calorimetry at 25 °C; Figure 5 and Table 7). Both values agree within the propagated error. Larger error of surface enthalpy for the data at 70 °C appears to be due to the last data point. The error of ΔH_{sln} of the finest sample is large (Figure 6). We choose the value 0.44 ± 0.04 J/m^2, obtained from acid calorimetry data at 25 °C, as being more accurate. The linear dependence of the calorimetric data (with the regression coefficient $R^2 = 0.96$) as a function of surface area shows that the total surface enthalpy is predominantly a function of surface area, with the other factor (e.g., structural change) being relatively minor.

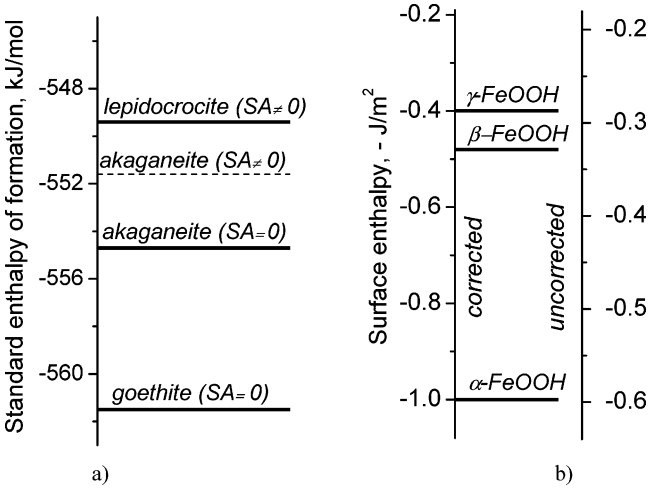

Figure 9. Schematic of (a) standard enthalpies of formation of goethite (α-FeOOH),[12] akaganeite (β-FeOOH), and lepidocrocite (γ-FeOOH),[22] and (b) negative surface enthalpies of goethite,[12] akaganeite, and lepidocrocite.[34] Data for corrected surface enthalpy of goethite and lepidocrocite are from work in preparation and are shown here to emphasize the general behavior. "SA" stands for "surface area".

Without taking into account the adsorption enthalpy and assuming the adsorbed water has the energetics of the liquid bulk water, the surface enthalpy of akaganeite is then 0.34 ± 0.04 J/m^2. This surface enthalpy represents the value for the surface of water-stabilized akaganeite. Thus, by adsorbing water akaganeite decreases its surface enthalpy by 0.1 J/m^2 (about 30%) as well as its total energy (eq 7):

$$FeOOH + xH_2O = FeOOH{\cdot}xH_2O + \text{heat (kJ/mol)} \quad (7)$$

Thus, many processes where akaganeite has been exposed to aqueous environment (soils, sediments, etc.) will be driven by energies of hydrated surface (e.g., ion exchange in solution, toxic element uptake from soils, transformations in aqueous solutions, etc.). Processes involving the "dry" akaganeite surface, controlled by energetics of dehydrated akaganeite, would include transformations in arid environments.

Although the surface enthalpy of akaganeite has not been reported before, we can discuss the consistency of our data by comparison with other iron oxy-hydroxides. As already discussed, oxy-hydroxide phases have lower surface enthalpy than the anhydrous phases[12] and, as the metastability increases, surface enthalpy decreases.[33] Akaganeite, being

(33) Navrotsky, A. *Geochem. Trans.* **2003**, *4*, 34.
(34) Majzlan, J. Thermodynamic of iron and aluminium oxides. Ph.D. Dissertation, University of California at Davis, Davis, CA, 2003.

less stable than goethite and more stable than lepidocrocite, indeed has surface enthalpy between those of lepidocrocite and goethite (Figure 9), following the trends mentioned above. Comparison with other iron oxides and transformations in the system as a function of increasing surface area will be given in future work.

Conclusions

Standard enthalpy of formation of akaganeite as function of particle size, β-FeOOH, surface enthalpy, and enthalpy of water adsorption is reported for the first time. Water adsorption experiments showed that about 40% of total excess water is stronger bound water with an integral enthalpy of adsorption of approximately -59 kJ/mol relative to water vapor or -15 kJ/mol relative to liquid water whereas the rest of the water is more weakly adsorbed water with liquid water energetics and enthalpy of adsorption of -44 kJ/mol (relative to vapor). Calculating surface enthalpy H_s and standard enthalpy of formation ΔH_f°, we corrected thermodynamic data for the energetics of the adsorbed surface water. The obtained value for the standard enthalpy of formation ΔH_f° is -554.7 ± 1.9 kJ/mol of FeOOH (zero surface area). The surface enthalpy H_s is 0.44 ± 0.04 J/m^2.

Acknowledgment. We acknowledge the National Center for Electron Microscopy at the Lawrence Berkeley National Laboratory for the use of its facilities. We thank S. Ushakov for TEM analysis and for the help with water adsorption experiments and M. Wang for SEM measurements. T. Dieckmann is thanked for the use of the freeze dryer. This work was supported by DOE Grant DEFG0397SF14749 and NSF Grant EAR 02-29332.

CM052543J